Inorganic Chemistry

Article

pubs.acs.org/IC

Ionothermal Synthesis of Tetranuclear Borate Clusters Containing *f*- and *p*-Block Metals

T. Gannon Parker, Amanda L. Chown, Austin Beehler, Divya Pubbi, Justin N. Cross, and Thomas E. Albrecht-Schmitt*

Department of Chemistry and Biochemistry, Florida State University, 95 Chieftain Way, Tallahassee, Florida 32306, United States

Supporting Information

ABSTRACT: The reactions of simple oxides or halides of trivalent lanthanides and actinides or bismuth with boric acid in the ionic liquid 1-butyl-3-methylimidazolium chloride at 150 °C result in the formation and crystallization of a series of isomorphous tetranuclear borate clusters with the general formula $M_4B_{22}O_{36}(OH)_6(H_2O)_{13}$ (M = La, Ce, Pr, Nd, Sm, Eu, Gd, Pu, and Bi). These clusters do not assemble with trivalent cations smaller than Gd^{3+}, suggesting that the formation of the clusters is dictated by the size of the metal ion. The cations are found in cavities along the periphery of a cage assembled from the corner- and edge-sharing interactions of BO_3 triangles and BO_4 tetrahedra, yielding a complex chiral cluster. Both enantiomers cocrystallize. The metal ions are nonacoordinate, and their geometries are best described as distorted tridiminished icosahedra. This coordination environment is new for both Pu^{3+} and Bi^{3+}. In addition to detailed structural information, UV/vis−NIR absorption and photoluminescence spectra are also provided.

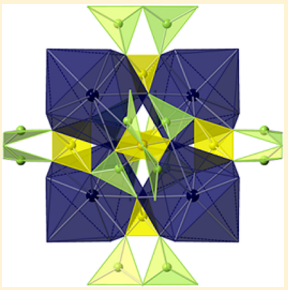

INTRODUCTION

Over the last few decades, ionic liquids, i.e., salts with melting points below 100 °C, have garnered considerable attention because of their unique properties. These include negligibly low vapor pressures, wide electrochemical windows, and exceptional tunability. The ability to exchange its cation or anion via facile ion exchange reactions has earned ionic liquids the title of "designer solvents" because their properties can be systematically tuned to achieve the properties desired from the solvent.[1−4]

Ionic liquids have numerous applications, such as dissolving cellulose and other forms of biomass,[5−9] acting as electrolytes for lithium batteries,[10−12] capturing and storing carbon dioxide,[13] and acting as extraction solvents for the separation of actinyl cations from acidic aqueous solutions. In the latter application, a hydrophobic ionic liquid has been utilized as an alternative to more flammable and volatile organic solvents such as kerosene or dodecane. To this end, ionic liquids have in some cases been shown to be as effective as or more effective than dodecane in the extraction of uranyl ions from acidic aqueous solutions when CMPO was used as an extractant. However, an ionic liquid has the drawback that its cation tends to leach into the aqueous phase through ion exchange processes.[14−19]

Ionic liquids are increasingly being employed as reactive solvents in the synthesis of inorganic framework materials, including zeolites and zeolite analogues.[20−27] These types of porous framework materials are typically synthesized by hydrothermal or solvothermal methods, but ionic liquids have proven to be attractive alternatives because the ionic liquid flux can act as both the solvent and the template for the framework, thus eliminating competition between solvent−framework and template−framework interactions.[20]

In an effort to understand more clearly the role of ionic liquids in the formation of templated 3D frameworks, we elected to expand on our previous work with lanthanide and actinide borates that were prepared by a hydrothermal or a boric acid flux method.[28−33] Because *f*-element borates have been studied extensively by our group, this would allow us to make direct comparisons among borates produced using hydrothermal, boric acid, and ionothermal flux methods.

In our previous work on the synthesis of borates using a boric acid flux, all structures were without exception polymeric, and they usually adopted a layered or a 3D framework topology.[34,35] On the basis of Morris's work on the ionothermal synthesis of zeolite analogues, it was expected that the ionothermal flux synthesis of lanthanide borates would lead to a layered or a framework structure with the cation of the ionic liquid serving as a charge-balancing and templating ion.[20,21]

However, rather than the expected extended structures, all of the reactions of lanthanides (Ln = La, Ce, Pr, Nd, Sm, Eu, and Gd) with boric acid in 1-butyl-3-methylimidazolium chloride ([Bmim][Cl]) resulted in isomorphous zero-dimensional tetrahedral tetranuclear metalloborate clusters with the molecular formula $Ln_4B_{22}O_{36}(OH)_6(H_2O)_{13}$. Interestingly, an analogous reaction with Pu(III) also led to a plutonium(III) borate cluster complex that is isomorphous with its 4*f* counterparts. This result is surprising not only because these compounds are the first examples of molecular *f*-element metalloborate clusters but also because they are all identical; in previous reactions in a boric acid flux, there were structural deviations not only between the 4*f* and 5*f* series but also among

Received: October 7, 2014
Published: January 2, 2015

DOI: 10.1021/ic502461d
Inorg. Chem. 2015, 54, 570−575

the neighboring 4*f* and 5*f* elements.[33] Finally, an analogous reaction was carried out with Bi(III) to confirm that cluster formation is dependent on the ionic radii of the metal ions,[36] and the bismuth analogue ($Bi_4B_{22}O_{36}(OH)_6(H_2O)_{13}$) formed as a result.

EXPERIMENTAL SECTION

La_2O_3 (99.99%, Aldrich), $CeCl_3{\cdot}7H_2O$ (99.9%, Aldrich), Pr_6O_{11} (99.9%, Aldrich), Nd_2O_3 (99.9%, Aldrich), Sm_2O_3 (99.9%, Alfa Inorganics), Eu_2O_3 (99.99%, Alfa Inorganics), Gd_2O_3 (99.9%, Aldrich), Bi_2O_3 (99.99%, Alfa Aesar), 1-chlorobutane (99.5%, Sigma-Aldrich), and 1-methylimidazole (99%, Aldrich) were used as received without further purification. 1-Butyl-3-methylimidazolium chloride was prepared according to the literature.[1] Plutonium (94% ^{239}Pu, 6% ^{240}Pu), in the form of plutonium(III) chloride, was supplied by Los Alamos National Laboratory. Because the $PuCl_3$ had oxidized to red $PuOCl_2$, it was first necessary to reduce $PuOCl_2$ to $PuBr_3$ by heating in 50 μL of concentrated HBr. Reactions were carried out in PTFE-lined stainless steel Parr 4749 acid-digestion vessels with internal volumes of 23 mL (for lanthanides and bismuth) or 10 mL (for plutonium). ***Caution!*** *^{239}Pu ($t_{1/2} = 2.411 \times 10^4$ years) represents a serious health risk because of its α and γ emission as well as the emission of its daughter isotopes. Weapons-grade plutonium also contains ^{240}Pu ($t_{1/2} = 6.56 \times 10^3$ years), which is also an α emitter. All studies with plutonium were conducted in a laboratory dedicated to studies of trans-uranic elements. This laboratory is located in a nuclear science facility and is equipped with HEPA filtered hoods and negative pressure gloveboxes that are ported directly into the hoods. A series of counters continually monitor radiation levels in the laboratory. The laboratory is licensed by the Nuclear Regulatory Commission. All experiments were carried out with approved safety operating procedures. All free-flowing solids are handled in gloveboxes, and the products are only examined when coated with either water or Krytox oil and water. There are significant limitations to accurately determine the yields of plutonium compounds because this involves processes that pose certain risks (drying, isolating, and weighing a solid) as well as manipulation difficulties resulting from the small quantities employed in the reactions.*

$M_4B_{22}O_{36}(OH)_6(H_2O)_{13}{\cdot}xH_2O$ (**M_4BO**, M = La−Nd, Sm−Gd, Bi, and Pu), Ln_2O_3 (Ln = La, Nd, and Sm−Gd), $CeCl_3{\cdot}7H_2O$, Pr_6O_{11}, Bi_2O_3, or $PuBr_3$ was loaded into a PTFE-lined stainless steel autoclave along with boric acid, [Bmim][Cl], and 20 μL of deionized water at a ratio of 1:6:15 (M/B/IL) for the lanthanide compounds or 1:12:15 for the plutonium compound. Water was omitted from the plutonium reactions because of the small quantities used; the residual water in the [Bmim][Cl] was adequate. The autoclave was sealed and heated at 150 °C for 5 days followed by cooling to room temperature at a rate of 5 °C/h. The products were then rinsed with ethanol to remove excess ionic liquid. Large colorless (or pale blue for plutonium) prismatic crystals suitable for X-ray diffraction were isolated in decent yield (Table 1). It should be noted that the crystals can be isolated in a much shorter time frame by instead heating at 150 °C for 24 h followed by cooling to room temperature at a rate of 10 °C/h; however, the longer protocol affords somewhat larger and better quality crystals. Additionally, although the reactions could all be run with either the metal oxides or the trihalides, the trihalides tended to give better yields with less residual starting material remaining upon completion of the reaction. Also, although all of these reactions were carried out using [Bmim][Cl] as the flux medium, experiments were also carried out using the ionic liquids 1-ethyl-3-methylimidazolium bromide ([Emim][Br]) and 1-butyl-3-methylimidazolium hexafluorophosphate ([Bmim][PF_6]). Reactions with [Emim][Br], which is a hydrophilic halide ionic liquid similar to [Bmim][Cl], gave the same cluster products. Reactions with hydrophobic [Bmim][PF_6], however, gave no crystalline product. Finally, reactions were carried out using cerium(IV) oxide and cerium(IV) sulfate, neither of which led to the formation of the desired crystalline product, indicating the importance of using a trivalent metal in these reactions.

Table 1. Crystallographic Data for La_4BO, Gd_4BO, and Pu_4BO[a]

compound	La_4BO	Gd_4BO	Pu_4BO
fw	1705.72	1779.08	2106.08
color and habit	colorless prism	colorless prism	pale blue prism
space group	*I*23 (No. 197)	*I*23 (No. 197)	*I*23 (No. 197)
a (Å)	18.111(1)	17.893(1)	17.852(1)
Z	2	2	2
T (K)	100	100	100
λ (Å)	0.71073	0.71073	0.71073
$R(F)$ for $F_o^2 > 2\sigma(F_o^2)$	0.062	0.060	0.101
$R_w(F_o^2)$	0.177	0.169	0.273

[a]Crystallographic data tables for **Ce_4BO**, **Pr_4BO**, **Nd_4BO**, **Sm_4BO**, **Eu_4BO**, and **Bi_4BO** can be found in the Supporting Information.

Crystallographic Studies. Single crystals of **M_4BO** (M = La−Nd, Sm−Gd, Bi, and Pu) were mounted on Mitogen mounts with viscous immersion oil and optically aligned on a Bruker D8 QUEST single-crystal X-ray diffractometer equipped with a 3-circle fixed-χ goniometer that used a digital camera. Initial intensity measurements were carried out using an IμS X-ray source with a 50 W microfocused sealed tube (Mo Kα, λ = 0.71073 Å) with high-brilliance and high-performance focusing multilayer optics. Quest software was used for the determination of unit cells and data collection control. The intensities of reflections of a sphere were collected by a combination of four sets of exposures (frames). Each set had a different φ angle for the crystal, and each exposure covered a range of 0.5° in ω. A total of 1464 frames were collected with an exposure time per frame of 10 s. The program SAINT was used for data integration, including Lorentz and polarization corrections. Semiempirical absorption corrections were applied using the program SCALE (SADABS).[37] The program suite SHELX-97 was used for space-group determination (XPREP), direct-methods structure solution (XS), imaging and peak assignment (XP), and least-squares refinement (XL).[38] All space-group determinations were checked using PLATON.[39] The final refinements included anisotropic displacement parameters for most atoms. The positions of hydrogen atoms could not be located in the Fourier difference map and were therefore omitted from refinement. In all structures, the inner-sphere-coordinated water molecules (O(1)) were refined isotropically, and the positions of their hydrogen atoms were not determined. The water molecules at the center of the clusters were refined anisotropically; again, the positions of the hydrogen atoms could not be determined. Disordered solvent water molecules were accounted for using the SQUEEZE protocol in PLATON. Atomic coordinates, bond distances, and additional information are provided in the CIF files (Supporting Information).

UV/Vis−NIR and Fluorescence Spectroscopy. UV/vis−NIR absorption data were acquired from single crystals of **M_4BO** (M = La−Nd, Sm−Gd, Bi, and Pu) using a Craic Technologies microspectrophotometer. Crystals were placed on quartz slides, and data were collected from 250 to 1150 nm. The exposure time was automatically optimized by the Craic software. Absorption data for **M_4BO** (M = La−Nd and Sm−Gd) can be found in the Supporting Information.

RESULTS AND DISCUSSION

Structure of $M_4B_{22}O_{36}(OH)_6(H_2O)_{13}{\cdot}xH_2O$ (M_4BO, M = La−Nd, Sm−Gd, Bi, and Pu). **M_4BO** crystallizes in the chiral cubic space group *I*23, and it is a molecular tetranuclear cluster complex (Figure 1). Over the course of the reaction, H_3BO_3 oligomerizes to form a cagelike moiety with an encapsulated water molecule at its core. The metal ions occupy the four cavities along the perimeter of the cage and are bridged via corner- and edge-sharing interactions with BO_3 triangles and BO_4 tetrahedra, respectively (Figure 2). They are each further coordinated by three water molecules, which leads to an overall

DOI: 10.1021/ic502461d
Inorg. Chem. 2015, 54, 570−575

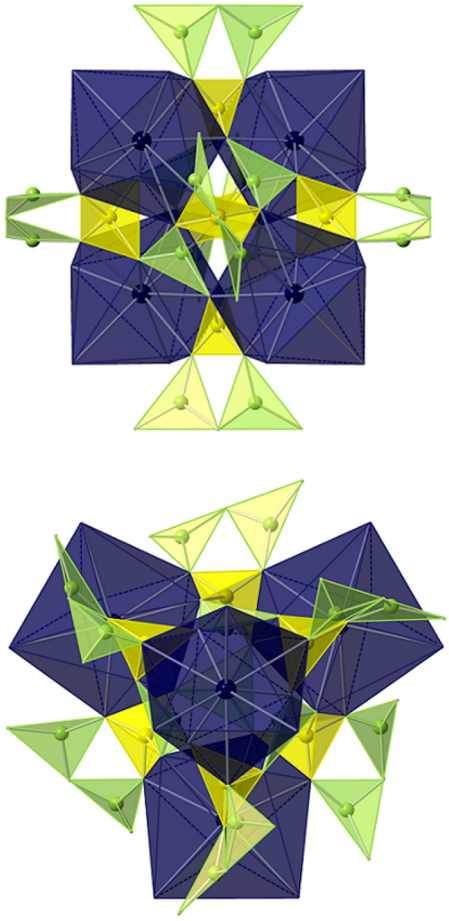

Figure 1. Polyhedral representation of $\mathbf{M_4BO}$ (M = La−Nd, Sm−Gd, Bi, and Pu) along the cluster's 2-fold rotational axis and 3-fold rotational axis (top and bottom, respectively). Blue polyhedra represent the nonacoordinate metal centers, light-green polyhedra BO_3 triangles, and yellow polyhedra BO_4 tetrahedra.

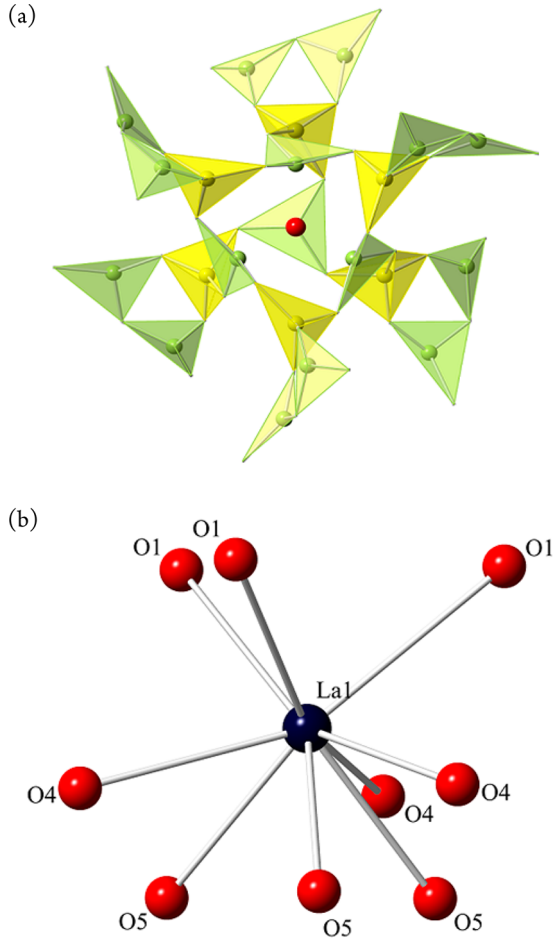

Figure 2. View of (a) the borate cage and the encapsulated water molecule and (b) the distorted tridiminished icosahedral geometry of the La center in $\mathbf{La_4BO}$, which is representative of all other $\mathbf{M_4BO}$ metal centers. Yellow tetrahedra represent BO_4 units, light-green triangles BO_3 units, and red spheres oxygen atoms.

nonacoordinate distorted tridiminished icosahedral geometry.[40] Average M−O bond lengths to the basal plane (M−O(5)) range from 2.439(3) Å for $\mathbf{Gd_4BO}$ to 2.547(6) Å for $\mathbf{La_4BO}$. The average bond length to the equatorial plane (M−O(4)) is 2.68(3) Å. Average bond lengths to the apical plane (M−O(1)) range from 2.733(6) Å for $\mathbf{Eu_4BO}$ to 2.837(6) Å for $\mathbf{La_4BO}$. An exhaustive list of bond lengths and angles can be found in the Supporting Information.

There is a large amount of void space between neighboring clusters that is likely occupied by distorted water molecules (Figure 3). Because there do not appear to be any [Bmim] cations in the void space, the clusters must be charge-neutral. Thus, in order to balance the charge on the cluster, 6 of the 12 terminal oxygen atoms along the perimeter of the cluster are presumed to be protonated, and the 3 terminal oxygen atoms coordinated to each metal center must be water molecules. This leads to an overall molecular formula of $M_4B_{22}O_{36}(OH)_6(H_2O)_{13}$ (M = La−Nd, Sm−Gd, Bi, and Pu).

Space-group determination for these cluster proved to be challenging because of the static disorder present in the structure. This disorder arises from the chirality of the clusters, with both enantiomers occupying equivalent positions with roughly 50% occupancy. This static disorder and the additional symmetry elements that the heaviest scattering elements suggest (a 4-fold rotoinversion axis and a mirror plane) might indicate that the correct space group is $I\bar{4}3m$, when in fact $I23$ yields the superior model. This is evident when point-group symmetry is taken into consideration for an individual cluster. When only a single enantiomer is examined, the 2-fold and 3-fold rotational axes of point group 23 are clearly visible, but the 4-fold rotoinversion axes and the mirror planes of point group $\bar{4}3m$ actually generate the opposite enantiomer (the disordered sites in the structure). Following this reasoning, two courses of action were available: (a) The structure could be solved in the higher-symmetry space group ($I\bar{4}3m$), and atoms B(1), O(2), O(4), and O(5) could be assigned 50% occupancy. (b) The structure could be solved in space group $I23$, and the disordered sites (corresponding to the opposite enantiomer) for B(1), O(2), O(3), and O(5) could be located in the Fourier difference map. By selecting option (b) and either assigning each of the disordered sites their own free variable or assigning each disordered site half occupancy, we achieved a model with a lower R_1 and more reasonable atomic displacement parameters than if option (a) were used. Choosing space group $I23$ thus appeared to give the best model for the crystal structure.

The size of the metal ion appears to play a key role in determining whether the clusters will form. Reactions were carried out in order to synthesize late lanthanide analogues of the clusters with Tb−Lu; in all cases, the reactions failed to produce the desired cluster product. It is likely that the reason

DOI: 10.1021/ic502461d
Inorg. Chem. 2015, 54, 570−575

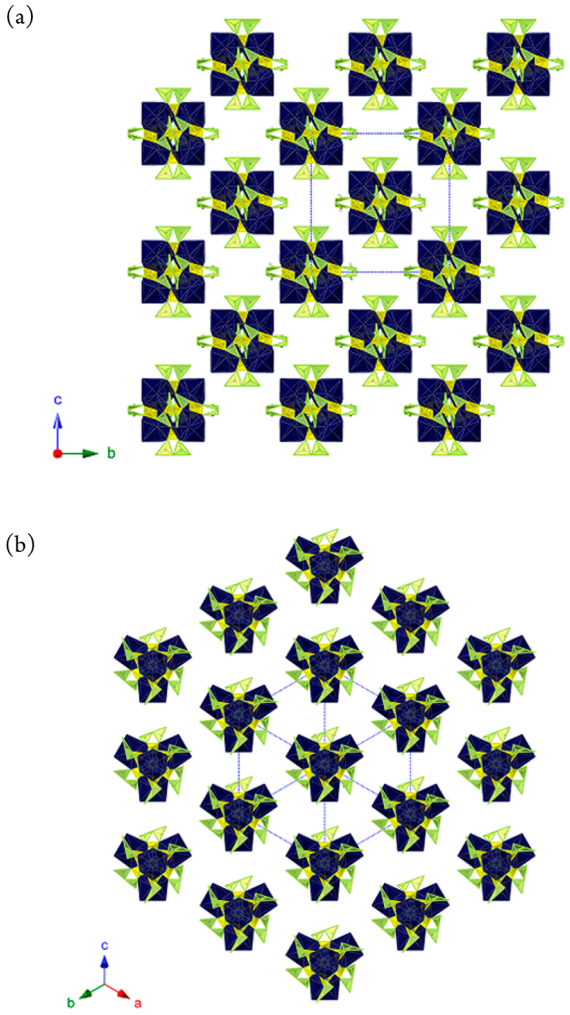

Figure 3. Views of M_4BO illustrating the packing of the clusters in the crystal structure: (a) normal to the *bc* plane and (b) normal to the (111) plane.

for this is that there is a threshold ionic radius for the metal ions, below which the ion will not effectively fit into the cavities of the borate cluster moiety. The effective ionic radius of nonacoordinate gadolinium(III) (1.107 Å) appears to be the lower limit. To test this hypothesis, reactions were run with yttrium(III), antimony(III), arsenic(III), chromium(III), and bismuth(III) oxides with the expectation that only the bismuth reaction would yield the target cluster product because it is the only ion of this group with a radius greater than that of gadolinium(III). This was indeed what was observed. It should be noted here that reproduction of the bismuth reaction is quite difficult, and the data that were obtained had high $R_{(int)}$ and R_1 values (0.1771 and 0.0938, respectively). These data are nonetheless included because of their value in the context of this report.

The formation of clusters rather than extended structures is especially surprising in this series of compounds because all of the lanthanide and actinide borates produced via hydrothermal or boric acid flux syntheses adopted either a 3D framework or a 2D sheet topology.[34,35] These compounds thus represent the first examples of molecular tetranuclear metalloborate cluster. The ionic liquid is presumably responsible for inhibiting the formation of an extended network, but the exact mechanism of how this is accomplished currently cannot be surmised with any degree of certainty. To confirm that the ionic liquid and not temperature was responsible for cluster formation (because these reactions were run at temperatures somewhat lower than those of previous borate reactions carried out by our group), reactions analogous to those described in the Experimental Section were carried out with the temperature varied over the range of 150−230 °C. It was found that the temperature did not affect the formation of crystalline product and that the same clusters formed over the entire range of temperatures. In fact, at 230 °C, the reaction with La_2O_3 resulted in more of the desired crystalline phase and no residual starting material. However, the decomposition of the ionic liquid is a function of reaction temperature and reaction time, and the residual ionic liquid in the products of the reactions carried out at elevated temperatures contained a much greater proportion of decomposed [Bmim][Cl], which was evident from the overwhelming ammoniacal odor.

The crystal structure of the plutonium analogue (**Pu_4BO**) proved to be especially enigmatic (Figure 4). The unit cell and

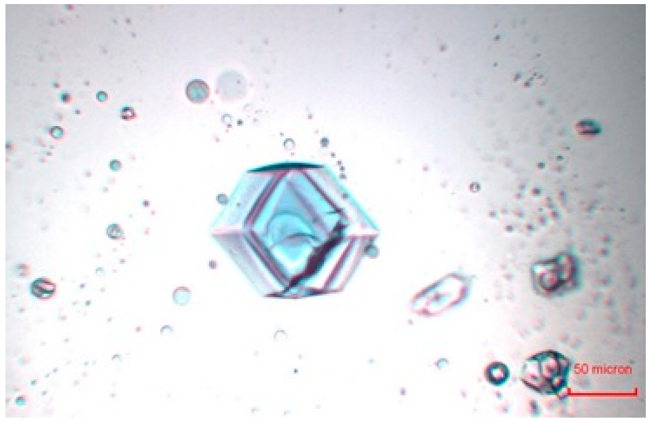

Figure 4. Photo of **Pu_4BO** illustrating its relatively large size, well-defined edges, prismatic habit, and lustrous blue color.

most of the structural features of the other clusters could be identified in the Fourier difference map; however, the peripheral BO_3 triangles (B(1), B(1)′, O(2), O(2)′, and O(3)) could not be located. This is likely because of the poor quality of the data ($R_{(int)}$ = 0.1974) and the heavy scattering of X-rays by the plutonium atoms, which makes identifying the significantly lighter boron and oxygen atoms exceedingly difficult. Additionally, the encapsulated water molecule that lies at the center of the cluster could not be located. In any case, the actual formula of the plutonium compound is likely to be the same as that of the lanthanide analogues because the unit cell parameters, habit, and identifiable structural features are consistent with those of its lanthanide counterparts.

UV/Vis−NIR and Fluorescence Spectroscopy. Absorption data were collected for all of the compounds. The spectrum of **La_4BO** expectedly shows no peaks in the range of 250−1150 nm, whereas that of **Ce_4BO** shows a strong absorption band centered around 325 nm, which is due to the well-documented $4f \rightarrow 5d$ transition.[41−44] A charge-transfer band centered around 314 nm was observed in the spectrum of **Eu_4BO**. Interestingly, the expected peaks that normally arise in the spectra of Eu^{3+} were not observed, and there is only one other peak apart from the charge-transfer band. It is centered around 398 nm and is presumably the $^5L_6$ peak. The spectra for other M_4BO compounds (M = Pr, Nd, Sm, Gd, and Pu) are in

DOI: 10.1021/ic502461d
Inorg. Chem. 2015, 54, 570−575

keeping with the literature, and the expected peaks are observed.[45]

The trivalent state for **Pu_4BO** is confirmed by the series of characteristic Laporte-forbidden *f*–*f* transitions that occur in the absorption spectrum between 250 and 1150 nm (Figure 5).

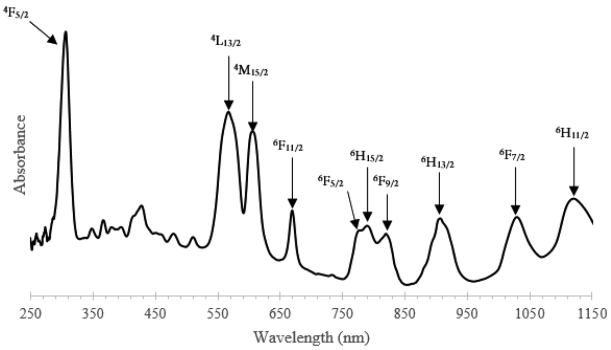

Figure 5. Absorption spectrum of **Pu_4BO**. The assigned peaks show *f*–*f* transitions that are consistent with trivalent plutonium.

The most intense peaks were assigned using the extensive analysis provided by Carnall and co-workers.[46] Plutonium(III) has a ground state of $^6H_{5/2}$, and the $^6H_{5/2} \rightarrow {}^6H_{13/2}$ transition that occurs around 900 nm is especially useful for distinguishing between plutonium(III) and plutonium(IV) because a transition in this region does not typically occur for plutonium(IV). The weaker peaks in the region of 328–528 nm could not be unambiguously assigned, and the labels for these peaks were intentionally omitted.

The emission spectrum of **Eu_4BO** was collected by irradiating a single crystal with 420 nm light, and the expected transition bands were observed in the region of 570–710 nm (Figure S6). These peaks are a result of the $^5D_0 \rightarrow {}^7F_J$ (J = 0–4) transitions of the metal ion and are consistent with previously reported spectra.

CONCLUSIONS

Herein, we have reported the ionothermal flux synthesis of a series of isomorphous tetranuclear metalloborate cluster complexes with the formula $M_4B_{22}O_{36}(OH)_6(H_2O)_{13}{\cdot}xH_2O$ (M = La–Nd, Sm–Gd, Bi, and Pu). These are the first examples of tetranuclear borate clusters of this type, and previous reactions with the trivalent lanthanides and actinides with boric acid using either hydrothermal or boric acid flux methods have exclusively yielded products with either 2D sheet or 3D framework topologies. The ionic liquid used as the flux solvent ([Bmim][Cl]) is presumably responsible for the inhibition of the formation of an extended borate network. This is potentially because the relatively large and asymmetrical imidazolium cations cannot adequately balance the charge and stabilize a highly charged anionic borate network. Additionally, previous reactions with trivalent lanthanides and actinides in hydrothermal and boric acid fluxes have shown differences in bonding and morphology between lanthanide and actinide borates as well as among lanthanide or actinide borates within a series, whereas when an ionothermal flux synthesis is used, identical morphologies are observed for all of the early lanthanides and plutonium.

Finally, it has been determined that the formation of the cluster is heavily dependent on both the oxidation state and the ionic radius of the metal ion. The electronic structure does not appear to play a significant role. This was confirmed by carrying out reactions with other trivalent cations with ionic radii less than or greater than that of gadolinium(III), the value of which is the suspected lower limit. Bi(III) and Pu(III) were found to be compatible with the formation of this cluster, which supports our hypothesis because the ionic radii of Bi(III) and Pu(III) align with those of the Ln(III) cations in the first half of the period. This type of change in chemistry has been noted in numerous chemical systems and is often called the gadolinium break.

It was originally proposed that an ionic liquid could be used to act as both the solvent and the template in the synthesis of new trivalent lanthanide and actinide borate frameworks. Although this result was not observed, we have shown that the effect of the ionic liquid on the products of reactions is not necessarily clear-cut and predictable in inorganic synthesis. However, even though the expected result was not observed, these results complement our previous work with ionothermal flux syntheses in that we have shown that an ionic liquid can be used to produce compounds that thus far have not been synthesized via more traditional methods, such as hydrothermal or solvothermal fluxes.[47]

ASSOCIATED CONTENT

Supporting Information

X-ray crystallographic files in CIF format for **M_4BO** (M = La–Nd, Sm–Gd, Bi, and Pu), selected bond lengths and angles, spectra, and crystallographic data tables. This material is available free of charge via the Internet at http://pubs.acs.org.

AUTHOR INFORMATION

Corresponding Author

*E-mail: albrecht-schmitt@chem.fsu.edu.

Notes

The authors declare no competing financial interest.

ACKNOWLEDGMENTS

We are grateful for support provided by the Chemical Sciences, Geosciences, and Biosciences Division, Office of Basic Energy Sciences, Office of Science, Heavy Elements Chemistry Program, U.S. Department of Energy, under Grant DE-FG02-13ER16414.

REFERENCES

(1) *Ionic Liquids in Synthesis*; Wasserscheid, P., Welton, T., Eds.; Wiley-VCH: Weinheim, Germany, 2002.
(2) Welton, T. *Chem. Rev.* **1999**, *99*, 2071.
(3) Wasserscheid, P.; Keim, W. *Angew. Chem., Int. Ed.* **2000**, *39*, 3772.
(4) Earle, M. J.; Seddon, K. R. *Pure Appl. Chem.* **2000**, *72*, 1391.
(5) Swatloski, R. P.; Spear, S. K.; Holbrey, J. D.; Rogers, R. D. *J. Am. Chem. Soc.* **2002**, *124*, 4974.
(6) Wang, H.; Gurau, G.; Rogers, R. D. *Chem. Soc. Rev.* **2012**, *41*, 1519.
(7) Fort, D. A.; Remsing, R. C.; Swatloski, R. P.; Moyna, P.; Moyna, G.; Rogers, R. D. *Green Chem.* **2007**, *9*, 63.
(8) Sun, N.; Rahman, M.; Qin, Y.; Maxim, M. L.; Rodríguez, H.; Rogers, R. D. *Green Chem.* **2009**, *11*, 646.
(9) Hassan, E.-S. R. E.; Mutelet, F.; Moïse, J.-C. *RSC Adv.* **2013**, *3*, 20219.
(10) Navarra, M. A. *MRS Bull.* **2013**, *38*, 548.
(11) Rock, S. E.; Wu, L.; Crain, D. J.; Sitaraman, K.; Roy, D. *ACS Appl. Mater. Interfaces* **2013**, *5*, 2075.
(12) Salem, N.; Abu-Lebdeh, Y. J. *J. Electrochem. Soc.* **2014**, *161*, A1593.

DOI: 10.1021/ic502461d
Inorg. Chem. 2015, 54, 570–575

(13) Bazhenov, S.; Mahinder, R.; Volkov, A.; Volkov, V.; Vlugt, T. J. H.; de Loos, T. W. *J. Chem. Eng. Data* **2014**, *59*, 702.
(14) Visser, A. E.; Rogers, R. D. *J. Solid State Chem.* **2003**, *171*, 109.
(15) Cocalia, V. A.; Jensen, M. P.; Holbrey, J. D.; Spear, S. K.; Stepinski, D. C.; Rogers, R. D. *Dalton Trans.* **2005**, 1966.
(16) Giridhar, P.; Vankatesan, K. A.; Srinivasan, T. G.; Vasudeva Rao, P. R. J. *J. Radioanal. Nucl. Chem.* **2005**, *265*, 31.
(17) Jensen, M. P.; Neuefeind, J.; Beitz, J. V.; Skanthakumar, S.; Soderholm, L. *J. Am. Chem. Soc.* **2003**, *125*, 15466.
(18) Visser, A. E.; Jensen, M. P.; Lazaki, I.; Nash, K. L.; Choppin, G. R.; Rogers, R. D. *Inorg. Chem.* **2003**, *42*, 2197.
(19) Binnemans, K. *Chem. Rev.* **2007**, *107*, 2592.
(20) Cooper, E. R.; Andrews, C. D.; Wheatley, P. S.; Webb, P. B.; Wormald, P.; Morris, R. E. *Nature* **2004**, *430*, 1012.
(21) Parnham, E. R.; Morris, R. E. *J. Mater. Chem.* **2006**, *16*, 3682.
(22) Wang, G.; Valldor, M.; Lorbeer, C.; Mudring, A.-V. *Eur. J. Inorg. Chem.* **2012**, *2012*, 3032.
(23) Wang, G.; Mudring, A.-V. *Crystals* **2011**, *1*, 22.
(24) Su, T.; Xing, H.; Xu, J.; Yu, J.; Xu, R. *Inorg. Chem.* **2011**, *50*, 1073.
(25) Nguyen, Q. B.; Lii, K.-H. *Dalton Trans.* **2011**, *40*, 10830.
(26) Lin, Y.; Dehnen, S. *Inorg. Chem.* **2011**, *50*, 7913.
(27) Byrne, P. J.; Wragg, D. S.; Warren, J. E.; Morris, R. E. *Dalton Trans.* **2009**, 795.
(28) Wang, S.; Alekseev, E. V.; Depmeier, W.; Albrecht-Schmitt, T. E. *Inorg. Chem.* **2011**, *50*, 2079.
(29) Polinski, M. J.; Alekseev, E. V.; Darling, V. R.; Cross, J. N.; Depmeier, W.; Albrecht-Schmitt, T. E. *Inorg. Chem.* **2013**, *52*, 1965.
(30) Polinski, M. J.; Wang, S.; Alekseev, E. V.; Cross, J. N.; Depmeier, W.; Albrecht-Schmitt, T. E. *Inorg. Chem.* **2012**, *51*, 11541.
(31) Polinski, M. J.; Pace, K. A.; Stritzinger, J. T.; Lin, J.; Cross, J. N.; Cary, S. K.; Van Cleve, S. M.; Alekseev, E. V.; Albrecht-Schmitt, T. E. *Chem.—Eur. J.* **2014**, *20*, 9892.
(32) Polinski, M. J.; Garner, E. B., III; Maurice, R.; Planas, N.; Stritzinger, J. T.; Parker, T. G.; Cross, J. N.; Green, T. D.; Alekseev, E. V.; Van Cleve, S. M.; Depmeier, W.; Gagliardi, L.; Shatruk, M.; Knappenberger, K. L.; Liu, G.; Skanthakumar, S.; Soderholm, L.; Dixon, D. A.; Albrecht-Schmitt, T. E. *Nat. Chem.* **2014**, *6*, 387.
(33) Polinski, M. J.; Grant, D. J.; Wang, S.; Alekseev, E. V.; Cross, J. N.; Villa, E. M.; Depmeier, W.; Gagliardi, L.; Albrecht-Schmitt, T. E. *J. Am. Chem. Soc.* **2012**, *134*, 10682.
(34) Wang, S.; Alekseev, E. V.; Depmeier, W.; Albrecht-Schmitt, T. E. *Chem. Commun.* **2011**, *47*, 10874.
(35) Polinski, M. J.; Alekseev, E. V.; Depmeier, W.; Albrecht-Schmitt, T. E. *Z. Kristallogr.—Cryst. Mater.* **2013**, *228*, 489.
(36) Shannon, R. D. *Acta Crystallogr.* **1976**, *A32*, 751.
(37) Blessing, R. H.; Sheldrick, G. M. *Acta Crystallogr.* **1995**, *A51*, 33.
(38) Sheldrick, G. M. *Acta Crystallogr.* **2008**, *A46*, 112.
(39) Spek, A. L. *J. Appl. Crystallogr.* **2003**, *36*, 7.
(40) Ruiz-Martínez, A.; Casanova, D.; Alvarez, S. *Chem.—Eur. J.* **2008**, *14*, 1291.
(41) Jacobs, R. R.; Krupke, W. F.; Weber, M. J. *Appl. Phys. Lett.* **1978**, *33*, 410.
(42) Pogatshnik, G. J.; Hamilton, D. S. *Phys. Rev. B* **1987**, *36*, 8251.
(43) Tanner, P. A. *Chem. Soc. Rev.* **2013**, *42*, 5090.
(44) Kalaji, A.; Mikami, M.; Cheetham, A. K. *Chem. Mater.* **2014**, *26*, 3966.
(45) Binnemans, K.; Görller-Walrand, C. *Chem. Phys. Lett.* **1995**, *235*, 163.
(46) Carnall, W. T.; Fields, P. R.; Pappalardo, R. G. *J. Appl. Phys.* **1970**, *53*, 2922.
(47) Parker, T. G.; Cross, J. N.; Polinski, M. J.; Lin, J.; Albrecht-Schmitt, T. E. *Cryst. Growth Des.* **2014**, *14*, 228.

DOI: 10.1021/ic502461d
Inorg. Chem. 2015, 54, 570−575